

Published in final edited form as:

J Neurochem. 2013 June ; 125(6): 869–884. doi:10.1111/jnc.12255.

***N*-Docosahexaenoylethanolamine is a potent neurogenic factor for neural stem cell differentiation**

Mohammad Abdur Rashid[§], Masanori Katakura^{§,+}, Giorgi Kharebava, Karl Kevala, and Hee-Yong Kim^{*}

Laboratory of Molecular Signaling, DICBR, NIAAA, NIH, 5625 Fishers Lane, Bethesda, MD, 20892-9410

Abstract

Docosahexaenoic acid (DHA) has been shown to promote neuronal differentiation of neural stem cells (NSCs) *in vivo* and *in vitro*. Previously, we found that *N*-docosahexenoyethanolamine (synaptamide), an endogenous DHA metabolite with endocannabinoid-like structure, promotes neurite growth, synaptogenesis and synaptic function. In this study, we demonstrate that synaptamide potently induces neuronal differentiation of NSCs. Differentiating NSCs were capable of synthesizing synaptamide from DHA. Treatment of NSCs with synaptamide at low nanomolar concentrations significantly increased the number of MAP2 and Tuj-1 positive neurons with concomitant induction of PKA/CREB phosphorylation. Conversely, PKA inhibitors or PKA knockdown abolished the synaptamide-induced neuronal differentiation of NSCs. URB597, a fatty acid amide hydrolase inhibitor, elevated the level of DHA-derived synaptamide and further potentiated the DHA- or synaptamide-induced neuronal differentiation of NSCs. Similarly, NSCs obtained from fatty acid amide hydrolase (FAAH) KO mice exhibited greater capacity to induce neuronal differentiation in response to DHA or synaptamide compared to the wild type NSCs. Neither synaptamide nor DHA affected NSC differentiation into GFAP-positive glia cells. These results suggest that endogenously produced synaptamide is a potent mediator for neurogenic differentiation of NSCs acting through PKA/CREB activation.

Keywords

synaptamide; neural stem cells; neurogenesis; docosahexaenoic acid; omega-3 fatty acids; PKA; CREB

Introduction

Docosahexaenoic acid (DHA, 22:6n-3), an omega-3 fatty acid highly enriched in the brain, is essential to maintain proper brain function (Salem et al., 2001; McNamara et al., 2006). Both human and animal studies have indicated that accretion of DHA at an early stage is particularly critical for optimal neurodevelopment. DHA not only plays a significant role as a structural component in neuronal membranes (Salem et al., 2001) but also participates in a variety of cellular events such as transcriptional activation (de Urquiza et al., 2000), cell

^{*}Correspondence: Hee-Yong Kim, Ph.D., Laboratory of Molecular Signaling, National Institute of Alcohol Abuse and Alcoholism, National Institutes of Health, 5625 Fishers Lane, Rm.3N-07, Bethesda, MD, 20892-9410, +1-301-402-8746 (Tel), +1-301-594-0035 (Fax), hykim@nih.gov.

[§]These authors equally contributed to this work and should be considered as co-first authors.

⁺Present address: Department of Environmental Physiology, Shimane University, Faculty of Medicine, 89-1 Enya-cho, Izumo, Shimane, 693-8501.

The authors have no conflict of interest to declare.

survival (Akbar et al., 2005) and maturation of developing neurons (Calderon and Kim, 2004; Cao et al., 2009).

It has been demonstrated that DHA promotes neurogenesis by stimulating neuronal differentiation of NSCs (Kawakita et al., 2006; Katakura et al., 2009; Ma et al., 2010). Kawakita et al. was the first to demonstrate that DHA promotes neurogenic differentiation in rat fetal NSCs as well as an *in vivo* model of neurogenesis (2006). The involvement of DHA in regulating expression of basic helix-loop-helix transcription factors and the cell-cycle has been implicated in this process (Katakura et al., 2009). Consistent with these results, an increase in hippocampal neurogenesis and improved spatial learning has been observed in fat-1 transgenic mice where the DHA level is elevated (He et al., 2009). Although these findings clearly demonstrated the neurogenic potential of DHA, it is not clear whether its endogenous metabolites are at least in part responsible for the observed induction of neuronal differentiation of NSCs.

N-docosahexaenylethanolamine is a member of the *N*-acylated amino acid or neurotransmitter class of lipid signaling molecules with endocannabinoid-like structure (Connor et al., 2010). Recently, we have observed that DHA is metabolized to *N*-docosahexaenylethanolamine in fetal neuronal cultures, and demonstrated that this metabolite is a potent mediator for neurite growth, synaptogenesis and glutamatergic synaptic activity (Kim et al., 2011a). According to its synaptogenic property and amide structure, the term 'synaptamide' was introduced for *N*-docosahexaenylethanolamine (Kim et al., 2011b). Synaptamide was detected in the brain and its endogenous level has been shown to be affected by diet (Kim et al., 2011a; Berger et al., 2001). For example, synaptamide increased in the brains of piglets after supplementation with DHA (Berger et al., 2001) while its level decreased in the fetal hippocampus when pregnant mice were fed an omega-3 fatty acid deficient diet (Kim et al., 2011a). Considering synaptogenic and neurotogenic properties of synaptamide, the DHA-dependent modulation of endogenous synaptamide levels may provide an explanation for the impediment in morphological development of neurons (Cao et al., 2009) as well as functional deficits observed with DHA-deficiency (Moriguchi et al., 2000). Nevertheless, the potential role of synaptamide in DHA-induced neuronal differentiation of NSCs has not been explored.

The aim of the present study was to determine whether synaptamide contributes to neuronal differentiation of NSCs. We found that first, DHA promotes neuronal differentiation of NSCs; second, DHA is metabolized to synaptamide in the cultured NSCs; third, synaptamide potently induces neuronal differentiation of NSCs; and fourth, the synaptamide-induced neuronal differentiation is mediated through PKA/CREB signaling.

Materials and Methods

Chemicals and antibodies

Dulbecco's Modified Eagle Medium/Ham's F12 (DMEM/F12 1:1) and insulin were purchased from Life Technologies Corporation (Carlsbad, CA, USA) and basic fibroblast growth factor (bFGF) from R&D Systems (Minneapolis, MN, USA). Glucose, HEPES, human apo-transferrin, progesterone, sodium selenite, putrescine, paraformaldehyde, heparin and forskolin were purchased from Sigma-Aldrich (St. Louis, MO, USA), and normal goat serum was acquired from Dako (Carpentaria, CA, USA). PKA inhibitor 6-22 amide was purchased from Calbiochem (EMD Millipore Bioscience, MA, USA) and H-89 was acquired from LC laboratories (Woburn, MA, USA). Anti-microtubule-associated protein 2 (MAP2) antibody and anti-glial fibrillary acidic protein (GFAP) antibody were purchased from Sigma-Aldrich (St. Louis, MO, USA). Antibodies to PKA, CREB and

GAPDH were purchased from Cell Signaling, and Tuj-1 was acquired from Millipore (CA, USA). Free fatty acids were obtained from Nuchek Prep Inc. (Elysian, MN).

Animals

Time pregnant female Wistar rats (gestation day 13) were obtained from Charles River Laboratories (Portage, MI, USA) and acclimated for a day before fetal brain was collected for NSC preparation. A minimum number of animals were used for the collection of fetal neural stem cells from anesthetized rats. All experiments in this study were carried out in accordance with the guiding principles for the care and use of animals approved by the National Institute on Alcohol Abuse and Alcoholism (LMS-HK31).

Fetal neural stem cell culture

NSCs were cultured by the neurosphere method (Rietze and Reynolds, 2006) modified by Katakura et al. (2009). Briefly, forebrain cortices of rats or FAAH wild type (+/+) or KO (-/-) mice (C57BL6/J) (Cravatt et al., 2001) were isolated on embryonic day 14.5 and 12.5, respectively. FAAH KO mice were kind gifts from Dr. Cravatt's laboratory. The cortices were mechanically disrupted into single cells by repeated pipetting in a serum-free conditioned medium (N2 medium) containing DMEM/F12 (1:1), 0.6% (wt/vol) glucose, 0.1125% (wt/vol) sodium bicarbonate, 2 mM L-glutamine, 5 mM HEPES, 100 µg/mL human apo-transferrin, 20 nM progesterone, 30 nM sodium selenite, 60 µM putrescine, and 25 µg/mL insulin. The dissociated cells were cultured in 6 cm dishes at a density of 1×10^5 cells/mL in N2 medium with 20 ng/mL bFGF and 2 µg/mL heparin in a humidified 5% CO₂/95% air incubator at 37 °C. Within 3–4 days, the cells grew as free-floating neurospheres that were then collected by centrifugation, mechanically dissociated by pipetting, and passaged. After the second passage, nestin- and SOX2-positive NSCs were enriched in the neurosphere (Supplemental Fig. 1A) with minimal presence of differentiated cells (MAP2-, Tuj-1 and GFAP-positive cells). The NSCs which were dissociated from the neurospheres and cultured for 3 h in the absence of FGF were mostly nestin- and SOX2-positive (Supplemental Fig. 1B), indicating the stemness of the NSC preparation.

Differentiation of NSCs

After the second passage neurospheres were mechanically dissociated and 5×10^5 cells/mL were plated onto 15 µg/mL poly-L-ornithine coated 6- or 24-well plates in N2 medium without bFGF and heparin to initiate the differentiation. The cultures were then treated with N2 medium containing polyunsaturated fatty acids (PUFA) bound to 0.05% (wt/vol) bovine serum albumin (BSA) and 40 µM vitamin E for 1–7 days as described earlier (Kim et al., 2000; Calderon and Kim, 2004). As the vehicle control, N2 medium containing 0.05% (wt/vol) BSA and 40 µM vitamin E was used.

Small hairpin RNA (shRNA) transfection

Transient transfections of NSCs were performed on the 4th day of plating under differentiating conditions. Lipofectamine 2000 reagent (Life Technologies Corporation) was used for this purpose according to manufacturer's instruction. Prior to the transfection, conditioned media from NSCs was removed, saved and replaced with fresh DMEM/F12. Lipofectamine/shRNA plasmid mixture was prepared in DMEM and added to the cells. After 4 h at 37 °C in a CO₂ incubator, the medium containing lipofectamine/shRNA plasmid mixtures was removed and replaced with original conditioned medium and the NSCs were treated with synaptamide for 72 h. Pre-designed HusH-29 shRNA sequences (Origene) used for PKA catalytic subunit knockdown were: GAGTGATGCTCGTGAAGCACAAGGAAAGT, and CCGAGATTATCCTGAGCAAAGGCTACAAC. The effectiveness of these shRNAs in

suppressing protein kinase A (PKA) expression was confirmed in NSCs by western blot analysis at 24h after transfection.

Immunofluorescence staining

For immunofluorescence staining, 2.5×10^5 NSCs were cultured in 0.5 mL media unless otherwise specified. Cultured cells were fixed with 4% (wt/vol) paraformaldehyde for 30 min at room temperature, washed with 0.1 M Tris-buffered solution (pH 7.5, TBS), blocked with 10% (vol/vol) normal goat serum in TBS containing 0.3% (vol/vol) Triton X-100 at room temperature for 60 min, and incubated with primary antibodies at 4 °C overnight. The primary antibodies were mouse anti-MAP2 (1:1000), mouse anti-neuron-specific class III beta-tubulin (Tuj-1, 1:1000), and rabbit anti-gial fibrillary acidic protein (1:2000). The cells were washed with TBS and incubated with Alexa Fluor 488- and 555- conjugated secondary antibodies (1:1000, Life Technologies Corporation) at room temperature for 60 min. To visualize nuclei, the cells were counterstained with 2 µg/mL 4',6-diamidino-2-phenylindole (DAPI). Finally, the cells were mounted with 80% (vol/vol) glycerol, visualized under a fluorescent microscope (IX81, Olympus Corp., Tokyo, Japan) and the image data were processed using MetaMorph (Molecular Devices, Sunnyvale, CA, USA) for quantitative information. The number of MAP2-, Tuj-1-, and GFAP-positive cells were counted from three separate wells with six to eight random fields per well for each individual experiment. At least three independent experiments were performed. The percentages of neuronal and glia cell population were calculated against the DAPI-positive total cell numbers which include undifferentiated stem cells and differentiated neurons and glia cells.

Western blot analysis

For western blot analysis, 1.25×10^6 NSCs were cultured in 2.5 mL media unless specified otherwise. Proteins in cell lysates (15 µg protein) were separated via SDS-PAGE and electroblotted onto a polyvinylidene difluoride (PVDF) membrane for 90 min at 100 V at 4 °C. The membranes were blocked with 5% BSA for 60 min in TBST (20 mM Tris-HCl, pH 7.5, 50 mM NaCl, 0.1% (vol/vol) Tween 20), and incubated overnight at 4 °C with primary antibodies in TBST. After being washed in TBST buffer, the membranes were incubated for 60 min in anti-rabbit or anti-mouse IgG-horseradish peroxidase (Santa Cruz Biotechnology, Santa Cruz, CA, USA) secondary antibodies diluted (1:2000) in TBST, and the labeled proteins were detected with chemiluminescence reagents (Thermo Fisher Scientific, Rockford, IL, USA). Unless specified otherwise, glyceraldehyde 3-phosphate dehydrogenase (GAPDH) was used as the loading control for all western blotting analyses. Western blot bands were quantified using a Kodak Gel Logic 440 imaging system with Image J software.

Cytotoxicity assay

To evaluate cytotoxicity, lactate dehydrogenase (LDH) released from NSCs was assayed using CytoTox 96 Non-Radioactive Cytotoxicity Assay kit (Promega, Madison, WI) according to the manufacturer's protocol. NSCs (2.5×10^5 NSCs in 0.5 mL media) were treated with different concentrations of synaptamide or DHA for 6 days. Fifty µL supernatant was collected from the culture, transferred to 96-well plates, and 50 µL of substrate solution was added. The enzymatic reaction was allowed to proceed for 30 min at room temperature, protected from light. After stopping the reaction by adding 50 µL/well of the stop solution, the absorbance was measured at 490 nm using a plate reader (Molecular Devices, Sunnyvale, CA). The released LDH activity was normalized to the total LDH activity determined from the cell lysate and supernatant. The final data were expressed as % of untreated control.

Analysis of synaptamide

For analysis of synaptamide, 2.5×10^6 NSCs were treated with 1 μ M DHA in the presence or absence of inhibitor. The cells and media were collected at the appropriate time points, lipids were extracted (Bligh and Dyer, 1959) and analyzed by HPLC-electrospray mass spectrometry using an Agilent 1290 UHPLC coupled to a TSQ Quantum Ultra mass spectrometer (Thermo Scientific, San Jose, CA) as described earlier (Kim et al., 2011a). Separation of synaptamide was achieved using a 50 mm \times 2.1 mm BDS Hypersil C18 column with a solvent gradient that consists of 0.1% (vol/vol) acetic acid in water/methanol varying from 70/30 to 0/100 over 1 min, and was then held for an additional 6 min. The column was re-equilibrated with 30% (vol/vol) methanol for 3 min between injections. For quantitation, the mass spectrometer was operated in the positive ion multiple reaction monitoring (MRM) mode using d_4 -synaptamide as an internal standard. Collision-induced dissociation (CID) was performed using argon as the collision gas at 1.5 mTorr with relative collision energy set at 15 V. Specific mass transitions were monitored based on the loss of ethanolamine (m/z 372 62, 376 66 and 394 62 for endogenous, d_4 - and $^{13}C_{22}$ -synaptamide, respectively) (Kim et al., 2011a).

Preparation of synaptamide

Stock solutions of DHA were made by dissolving the fatty acid in methanol. Synaptamide (d_0 - and d_4 -synaptamide) was prepared as described previously (Kim et al., 2011). In brief, 100 mg of DHA-chloride (Nuchek Prep Inc., Elysian, MN) was dissolved in cold methylene chloride (Sigma-Aldrich, St. Louis, MO) followed by drop-wise addition of 100 μ L of d_0 - (Sigma-Aldrich, St. Louis, MO) or d_4 -ethanolamine (Cambridge Isotope Laboratories, Andover, MA). The mixture was allowed to react 20 min on ice, washed 4 times with 20 mL LC/MS grade water, dried under nitrogen, and resuspended in LC/MS grade methanol. Product purity (>98%) was assessed using positive and negative ion mode ESI mass spectrometry and by gas chromatographic analysis after trimethylation with BF_3 (Sigma-Aldrich, St. Louis, MO) as described earlier (Wen and Kim 2004).

Statistical analysis

The results are expressed as means \pm SD for triplicate samples and represent at least three independent experiments. Statistical analyses were conducted using Student's *t* test and in some cases one-way ANOVA followed by Bonferroni-corrected pairwise comparisons. Unless indicated otherwise, a *p* value of less than 0.05 (Student's *t* test) or 0.01 (Bonferroni) was considered significant.

Results

Effects of long chain PUFA on differentiation of NSCs

The nervous system is highly enriched with long chain PUFAs including DHA and arachidonic acid (AA). Also, when the DHA level is reduced in the brain by dietary omega-3 fatty acid depletion, a compensatory increase of docosapentaenoic acid (DPA_n-6) is known to occur (Galli et al., 1971). Therefore, we first examined the effects of DHA, AA and DPA_n-6, on the neuronal differentiation of NSCs in comparison to oleic acid (OA)-treated or unsupplemented NSCs. Cultured NSCs were incubated with 1 μ M long chain PUFA in the absence of bFGF for 7 days and the expression of MAP2 and Tuj-1 (neuron markers), and GFAP (astrocyte marker) were examined by immunocytochemistry (Fig. 1A and B) and western blot analysis (Fig. 1C and D). The number of MAP2 and Tuj-1 positive cells was significantly increased after incubation with DHA (from 10.5 ± 2.5 to 25.2 ± 3.6 %, $p < 0.001$ for MAP2 and from 13.8 ± 3.3 to 30.0 ± 4.5 %, $p < 0.001$ for Tuj-1 positive cells, respectively) and to a lesser degree with DPA_n-6 (to 19.9 ± 2.8 %, $p < 0.01$ for MAP2

and $23.2 \pm 3.7\%$, $p < 0.05$ for Tuj-1 positive cells, respectively). However, AA or OA produced no effects. None of these fatty acids affected the number of GFAP positive cells. The expression pattern for MAP2, Tuj-1 and GFAP proteins shown by the western blot analysis (Fig. 1C and D) was consistent with the microscopic data. DHA was more effective than DPAn-6 in increasing MAP2 and Tuj-1 protein levels while AA and OA showed no significant effects (Fig. 1C and D). None of these lipids altered the GFAP protein level. These data confirmed the established effects of DHA on neuronal differentiation of NSCs while demonstrating DPAn-6 as a considerably weaker substitute for DHA in terms of neurogenic function.

Metabolism of DHA to synaptamide in cultured NSCs

Since the conversion of DHA to synaptamide has been observed in hippocampal neuronal cultures (Kim et al., 2011a), we examined whether this also occurs in NSC cultures under differentiating conditions. When the NSCs were incubated with unlabeled DHA or $^{13}\text{C}_{22}$ -DHA, the formation of synaptamide was detected from both substrates (Fig. 2). The MRM approach using mass transition from the intact molecule (MH^+) to ethanolamine based on the specific fragmentation at the amide bond allowed quantitative determination of synaptamide with high specificity in the presence of the deuterium labeled internal standard. The production level of synaptamide was estimated to be 40.2 ± 3 fmol when approximately one million NSCs were treated with total $1\ \mu\text{M}$ DHA and $^{13}\text{C}_{22}$ -DHA for 4 days under differentiating conditions.

Neuronal differentiation of NSCs induced by synaptamide

Once the production of synaptamide from DHA by NSCs was confirmed, we examined the effect of synaptamide on the neuronal differentiation of NSCs. NSCs were treated with synaptamide in the $1\text{--}500$ nM range for 7 days, and differentiation was evaluated by immunostaining coupled to fluorescence microscopy along with western blot analysis. The immunofluorescence staining data (Figs. 3A and B) showed significant increases in MAP2 (from 9.9 ± 1.0 to $14.9 \pm 2.1\%$, $p < 0.01$) and Tuj-1 positive cells (from 10.3 ± 1.1 to $16.9 \pm 3.5\%$, $p < 0.01$) after treatment with synaptamide at a concentration as low as 1 nM, while differentiation into GFAP positive cells was not affected. Consistent with these results, western blot analysis showed significant increases in both MAP2 and Tuj-1 protein levels after treatment with as low as 1 nM synaptamide (Figs. 3C and D), indicating that synaptamide is a potent neurogenic factor. No significant differences in the GFAP protein level were observed. Neuronal differentiation examined over a wide range of synaptamide concentration revealed a bell shaped dose-response relationship (Fig. 3B). The maximum effect of synaptamide on neuronal differentiation was reached at a concentration of 10 nM, and the response gradually diminished above this concentration. The western blot analysis also confirmed the immunostaining results as MAP2 and Tuj-1 protein levels were lower at 100 nM in comparison to 10 nM synaptamide (Figs. 3C and D, Supplemental Fig. 2C and D). The DHA-induced neuronal differentiation also showed a similar bell shaped dose-response relationship with the peak response at around $1\ \mu\text{M}$ (Supplemental Fig. 2). Synaptamide was by $50\text{--}100$ fold more effective than DHA in inducing NSC differentiation into Tuj-1 and MAP2-positive neurons (Supplemental Fig. 2A, B). Consistently, Tuj-1 protein expression peaked at 10 nM and $1\ \mu\text{M}$ of synaptamide and DHA, respectively, and decreased at higher concentrations (Supplemental Fig. 2C, D). Since the maximal effect of synaptamide was observed at 10 nM, this concentration was used to test neuronal differentiation of NSCs in most of the experiments.

Involvement of PKA/CREB activation in synaptamide-induced differentiation of NSCs

To explore the mechanisms underlying the synaptamide-induced neuronal differentiation of NSCs, we screened several key kinase pathways using the kinome profiling approach

(Parikh et al., 2009) and found that synaptamide increases phosphorylation of PKA substrates (data not shown). Synaptamide showed negligible effects on the substrates for other kinases such as Akt, PLK, CKII and ATM, although possible involvement of these pathways cannot be completely excluded (data not shown). To determine whether the PKA signaling pathway is involved in synaptamide-induced neuronal differentiation, NSCs were treated with 10 nM synaptamide for 7 days in the absence or presence of PKA inhibitors, H89 or PKA inhibitor 6–22 amide, and differentiation was evaluated by immunocytochemistry and western blot analysis. Forskolin, an activator of adenylate cyclase and thus PKA signaling (Seamon et al., 1981), was used as a positive control. The immunocytochemical analysis (Fig. 4A and B) showed that synaptamide at 10 nM and forskolin at 1 μ M similarly increased the percentage of MAP-2 (by 1.6- and 1.9-fold, respectively) and Tuj-1 positive cells (by 2.0- and 2.3-fold, respectively), but the observed increases were abolished by the PKA inhibitors H89 or PKA inhibitor 6–22 amide. Western blot results also indicated that MAP2 and Tuj-1 expression as well as cAMP response element binding protein (CREB) and PKA phosphorylation were upregulated by synaptamide and forskolin and this increase was prevented by the PKA inhibitors (Figs 4C and D). None of these treatments significantly altered the percentage of GFAP positive cells or GFAP protein level. These results indicate that synaptamide-induced neuronal differentiation of NSCs requires activation of the PKA/CREB signaling pathway.

Effects of PKA knockdown on synaptamide-induced neuronal differentiation of NSCs

To provide further evidence for the involvement of PKA in synaptamide-induced NSC differentiation, the effects of PKA knockdown on neuronal differentiation was examined (Fig. 5). We used vectors coexpressing green fluorescent protein (GFP) and shRNAs that are targeted to knockdown the PKA catalytic subunit (GFP-PKA shRNA) or scrambled shRNA (GFP-Sc shRNA). We first validated the effectiveness of these shRNAs in suppressing PKA expression by western blot analysis using Neuro 2A cells after 24h of transfection (Fig. 5A). In comparison to the scrambled shRNA, both PKA shRNAs clearly decreased the PKA level. NSCs were transfected with these silencing vectors and subsequently treated with either vehicle (DMSO) or 10 nM synaptamide for 72h, and differentiated neurons were immunostained using MAP2 antibody (visualized in red) (Figs. 5B and 5D). Neuronal differentiation was evaluated by the percentage of MAP2-positive neurons among at least 100 shRNA-expressing cells (visualized in green) per sample (Fig. 5C). As shown in the representative micrographs (Fig. 5B, far left panel; Fig. 5D top panel), GFP-Sc shRNA expressing cells were identified in both neuronal (GFP, MAP2-overlapping cells which were circled in white) and non-neuronal cell populations. Synaptamide treatment significantly increased MAP2-positive neurons within the GFP-Sc shRNA-expressing cell population (from 16% at the basal condition to 32% after synaptamide treatment, $p < 0.001$) (Fig. 5A, second panel from left; Fig. 5D, second panel from top). PKA knockdown did not alter the percentage of MAP2 positive neurons in vehicle-treated control (16 and 15% for Sc shRNA- and PKA shRNA-expressing cells, respectively; micrographs not shown). However, PKA shRNA abolished the synaptamide-induced increase in MAP2 positive cells seen in the Sc shRNA-expressing cells (12 % vs. 32% for PKA shRNA- vs. Sc shRNA-expressing cells, $p < 0.001$) (Fig. 5A, third and fourth panels from left; Fig. 5D, third and fourth panels from top). Both PKA shRNA plasmids produced similar inhibitory effects. These results further established the critical role of PKA signaling in synaptamide-induced neuronal differentiation of NSCs.

Effects of fatty acid amide hydrolase on DHA-derived synaptamide levels during differentiation

Because synaptamide is a substrate for fatty acid amide hydrolase (EC 3.5.1.99, FAAH) (Kim et al., 2011a), the level of synaptamide and its neurogenic capacity can be regulated by

the FAAH activity. Therefore, we first examined the expression profile of FAAH in NSCs by western blotting, and the effect of FAAH inhibition on DHA-derived synaptamide accumulation using tandem mass spectrometry (Fig. 6). FAAH was detected in NSCs from the first day of differentiation, and its expression level increased considerably by the day 4 in culture (Fig. 6A). Accordingly, the level of synaptamide derived from 1 μ M DHA gradually declined during the course of differentiation (from 148.6 ± 3.8 fmol/ 2.5×10^6 NSCs on day 1 to 95.6 ± 10.7 , $p < 0.001$ and 49.4 ± 0.4 , $p < 0.001$ fmol/ 2.5×10^6 NSCs for day 4 and 7, respectively). Addition of 20 nM URB597 to the culture media to prevent the hydrolysis significantly elevated the synaptamide level at all time points examined. The synaptamide level peaked on day 4, and then decreased by day 7 to a level similar to that on day 1 even in the presence of URB597, suggesting that degradation pathways other than hydrolysis by FAAH are operational during the course of NSC differentiation. Alternatively, it is possible that the production rate of synaptamide was reduced by day 7.

Effects of FAAH inhibition on DHA- or synaptamide-induced NSC differentiation

Significant FAAH activity identified in NSCs suggested that elevating the synaptamide level by suppressing FAAH activity may enhance synaptamide-induced neuronal differentiation of NSCs. We tested this proposition by two different approaches; employing FAAH inhibitors or a FAAH KO mouse model (Fig. 7). To this end, less than optimum concentrations of DHA (100 nM) and synaptamide (5 nM) were deliberately chosen to examine the effects of elevated synaptamide levels on neuronal differentiation (Supplemental Fig. 2A, B). The NSC cultures were treated with URB597 for 30 min, and subsequently with DHA or synaptamide for 7 days, and neuronal differentiation was evaluated by immunocytochemistry (Fig. 7 A and B) and western blotting (Fig. 7C and D). Immunocytochemical analysis showed that both DHA and synaptamide significantly increased MAP2 positive neurons (approximately 1.7- and 2.3-fold increase compared to control, respectively). The percentage of MAP2 positive cells was further increased when URB597 was included in the culture (approximately 2.2- and 3.1-fold increase compared to control, respectively) without affecting GFAP positive cells. Consistent results were obtained by western blot analysis; pretreatment with 20 nM URB597 significantly enhanced the DHA- and synaptamide-induced increase in MAP2 and Tuj-1 levels, as well as the phosphorylation of PKA and CREB.

The effect of FAAH was further confirmed using NSCs prepared from a mouse model devoid of FAAH expression. As observed with rat NSCs, the NSCs from fetal mouse brains also showed significant increases in neuronal differentiation in response to DHA and synaptamide. The NSCs from FAAH KO mice showed more MAP2-positive cells (Fig. 7E and F) and enhanced PKA phosphorylation (Fig. 7G) after 7 days of incubation with DHA or synaptamide in comparison to those from the wild type animals. The observation that the neurogenic differentiation capacity of synaptamide or DHA is regulated by FAAH activity together with the NSCs' ability to produce synaptamide (Figs. 2 and 6) from DHA as well as potent neurogenic activity of synaptamide (Fig. 3) provides strong evidence that synaptamide is a mediator for DHA-induced neuronal differentiation of NSCs.

Discussion

In the present study, we demonstrated that synaptamide is a potent neurogenic factor, mediating DHA-induced neuronal differentiation of NSCs. We found that NSCs can metabolize DHA to synaptamide that induces neuronal differentiation at a significantly lower concentration than DHA. We also demonstrated that PKA-CREB signaling is necessary for the synaptamide-induced neuronal differentiation of NSCs. Schematic depiction of the signaling pathway for DHA-induced neuronal differentiation of NSCs is shown in Figure 8.

Among the several fatty acids examined, DHA and DPAn-6 specifically induced neuronal differentiation of the NSCs (Fig. 1). Treatment of tertiary neurospheres, termed as gliogenic neural stem cells, with 0.1 μM of DHA has been reported to increase the number of Tuj-1 positive cells but not GFAP positive cells (Sakayori et al., 2011). We used secondary neurospheres where MAP2- or Tuj-1 positive cells were derived at 8–17% of NSCs, while 15–24% developed into GFAP positive cells after 7 days of differentiation. Apparently, the properties of NSCs used in the present study were similar to those of the tertiary neurospheres from the previous study in that increases in neuronal differentiation were observed after DHA treatment (Lim et al., 2005). DPAn-6 is known to reciprocally replace DHA when DHA is lost in the brain as in the case of dietary deprivation of omega-3 fatty acids (Galli et al., 1971).

Nevertheless, numerous findings indicated that DPAn-6 can sufficiently support neither neuronal survival and development nor brain function (Moriguchi et al., 2000; Calderon and Kim, 2004; Akbar et al., 2005; Lim et al., 2005). Our observation that DPAn-6 is less effective than DHA despite its ability to induce neuronal differentiation of NSCs (Fig. 1) also suggests an adverse impact of DHA-depletion on neurodevelopment.

We have previously found that synaptamide is synthesized from DHA in hippocampal neuronal cultures and its content in the fetal hippocampus is decreased by feeding pregnant mice an omega-3 fatty acid deficient diet (Kim et al; 2011a). We also demonstrated that synaptamide is the principal mediator for DHA-induced neuritogenesis and synaptogenesis in primary hippocampal neurons (Kim et al; 2011a). The present study demonstrates the metabolism of DHA by NSCs to synaptamide (Fig. 2) which potentially increases the percentage of MAP2 and Tuj-1 positive cells and the expression levels of these neuronal marker proteins (Fig. 3). The effective concentrations of synaptamide (low nM range) appear to be attainable under physiological conditions. Although the exact cellular concentration of synaptamide at a given moment cannot be determined, 4–12 nM can be reached based on 50–150 fmole synaptamide produced from 1 μM DHA incubated with 2.5 million NSCs (Fig. 6B) if the estimated cell volume of 5 pL/cell is applied (Korchev et al., 2000). Moreover, the basal DHA concentration in the brain was found to be low μM (Contreras et al., 2000), sufficient to produce nM concentrations of synaptamide. In addition, suppression of synaptamide hydrolysis by using URB597 or FAAH KO increased the synaptamide content (Fig. 6) and potentiated DHA- and synaptamide-induced neuronal differentiation (Fig. 7). Taken together, these findings indicate that synaptamide is likely an endogenous and physiologic neurogenic factor which is dependent on DHA availability.

DHA-derived neuroprotection has been well-documented (Akbar et al., 2005; Bazan, 2006; Kim et al., 2010), and therefore, the promoted neuronal differentiation observed in DHA-treated NSCs may be due to its neuroprotective effects. However, significant reduction of cytotoxicity was observed only at 1 μM DHA among many effective concentrations while decreased LDH activity was not observed at any of the synaptamide concentrations tested (Supplemental Fig. 3), suggesting that synaptamide and DHA promote neurogenic differentiation via mechanism other than neuroprotection. In addition, the bell shaped dose-response relationship was similar for both synaptamide and DHA with the former more effective than the latter by approximately 50–100 fold (Supplemental Fig. 2). These data strongly support the interpretation that synaptamide production at least in part mediates the DHA-induced neuronal differentiation of NSCs. The LDH assay indicated that cytotoxicity increased only at the highest concentrations tested, i.e., 1000 nM synaptamide and 5000 nM DHA (Supplemental Fig. 3). It was intriguing to observe that the response declined above 10 nM synaptamide and 1 μM DHA even though there was no significant increase in cytotoxicity. The reason for the diminished capability to induce neuronal differentiation at

higher concentrations of synaptamide and DHA is not clear at present and warrants further investigation.

Numerous studies have indicated the involvement of cAMP/PKA/CREB signaling pathway in NSC differentiation (Kim et al., 2002; Lonze et al., 2002; Chu et al., 2006; Wang et al., 2007; Lepski et al., 2010). Many upstream signaling pathways including cAMP-PKA, Mitogen-activated Protein Kinase, Phospholipase C/protein kinase C and Ca²⁺/calmodulin-dependent protein kinases II/IV can lead to CREB activation (Johannessen et al., 2004). Apparently, cAMP/PKA signaling was responsible for the synaptamide-induced neuronal differentiation of NSCs observed in this study, since synaptamide increased phosphorylation of PKA and CREB, while inhibiting PKA activation or PKA knock down virtually abolished synaptamide-induced neuronal differentiation (Figs. 4 and 5). The observed induction of neuronal differentiation by forskolin, a cAMP/PKA activator (Fig. 4), also supports the involvement of this pathway. Previously, increasing cAMP by forskolin has been reported to increase the number of progenitor cells adopting a neuronal phenotype (Palmer et al., 1997).

Potential target genes of CREB include the brain derived neurotrophic factor (BDNF) which is known to enhance the survival of newborn neurons in vitro and in the adult dentate gyrus (Lee and Son, 2009) and NeuroD, a neurogenic transcription factor (Lee, 1997; Jagasia et al., 2009). It has been reported that DHA improves learning and memory function via BDNF and CREB activation (Wu et al., 2011) and increases NeuroD mRNA expression in cultured NSCs (Katakura et al., 2009). Consistent with these results, DHA depletion in the brain has been shown to reduce the proteins which are downstream targets of CREB (Sidhu et al., 2011). These previous findings as well as our current data support a role of DHA-derived synaptamide in neuronal differentiation of NSCs via CREB-dependent transcriptional activation.

The endogenous receptor mediating synaptamide effects is currently unknown. Several receptors for synaptamide-induced differentiation could be considered such as G protein coupled receptor (GPR) 40, cannabinoid receptor type 1 (CB1), retinoid X receptor (RXR) and peroxisome proliferator-activated receptors (PPARs), however, there are factors that tend to exclude each of these possibilities. It has been reported that GPR40 is expressed in the brain and pancreas in the human and monkey, and its ligands are medium- and long-chain fatty acids including DHA, EPA, and AA. GPR40 is also expressed in the subgranular zone of the adult monkey hippocampus where neurogenesis is stimulated by GPR40-CREB signaling (Ma et al., 2008). Although DHA has been shown to increase neuronal differentiation in rat NSCs transfected with GPR40 (Ma et al., 2010), GPR40 expression has not been demonstrated in rodents thus far.

Synaptamide has structural similarity with anandamide (AEA), an endogenous ligand for CB receptors. Therefore, it is possible that CB1, the major CB receptor form expressed in the brain, may mediate synaptamide induced-PKA-CREB activation. It has been shown that CB1 is expressed in neural progenitor cells (NPCs) from post-natal day 4 mouse brain where AEA stimulates CREB phosphorylation and increases neuronal differentiation of NPCs in 7 days (Soltys et al., 2010). However, HU210, a potent CB agonist, and AEA are reported to promote proliferation but exert no significant effects on neuronal differentiation of NSCs obtained from fetal brains at embryonic day 17, at which time CB1 expression was detected (Jiang et al., 2005). The NSCs used in our study were obtained from rat fetal brain at embryonic day 14.5 when CB1 expression was minimal. Furthermore, the affinity of CB receptors for synaptamide is much weaker than for AEA (Sheskin et al., 1997), suggesting unlikely involvement of CB1 in the potent action of synaptamide on neuronal differentiation of NSCs observed in the present study.

PPARs are expressed in the NSCs and may also play a role in proliferation and differentiation of NSCs (Cimini and Ceru, 2008). Involvement of PPAR in NSC proliferation and differentiation has been reported; however, a PPAR agonist was found to inhibit neuronal differentiation of NSCs (Morales-Garcia et al., 2011; Wada et al., 2006). *N*-acylethanolamines (NAE) activate PPAR, but synaptamide showed rather minor activity in comparison to oleoylethanolamide, linolenylethanolamide and AEA (Artmann et al., 2008). Furthermore, we found no effects of OA and AA on neuronal differentiation of the NSCs at low μM concentrations (Fig. 1), despite the capability of NSCs to convert these fatty acids to the corresponding NAEs (data not shown). These findings argue against the role of PPARs in synaptamide-induced neuronal differentiation of NSCs.

DHA is an endogenous ligand for RXR (de Urquiza et al., 2000), and other fatty acids including AA have been shown to bind to RXR (Lengqvist et al., 2004). RXRs are expressed in the NSCs, and pre-activation of retinoid signaling has been shown to facilitate neuronal differentiation of mesenchymal stem cells (Bi et al., 2010). Nonetheless, AA did not affect the neuronal differentiation of NSCs in our study. Moreover, according to the RXR ligand binding assay, the DHA concentration that enables RXR activation is much higher than the concentration that induces hippocampal neurite growth (Calderon and Kim, 2007) or neuronal differentiation of NSCs seen in this study. However, ligand binding assays may not be adequate to address the cellular signaling transmitted through RXR activation. It is possible that RXR signaling depends on not only the extent of ligand binding but also the type of ligands and dimerization partners, which in turn may determine sensitivity and characteristics of RXR transcriptional activity *in vivo*. Therefore, the possible role of RXR activation in DHA- or synaptamide-induced neuronal differentiation of NSCs may need to be further investigated.

In conclusion, the present study demonstrates that synaptamide is a potent mediator for promoting neuronal differentiation of NSCs. The neurogenic property of synaptamide was found to be transmitted through PKA-CREB signaling. Although the biosynthetic pathway is yet to be determined, synaptamide is derived from DHA in NSCs. Therefore, the neurogenic capacity of NSCs during development can be directly linked to the endogenous synaptamide level which in turn is dependent on the dietary omega-3 fatty acid intake that influences the brain DHA content. Obviously, further research efforts are necessary to determine the specific receptor and downstream target genes of synaptamide, as well as the biosynthetic mechanisms for this DHA-derived potent neurogenic factor.

Supplementary Material

Refer to Web version on PubMed Central for supplementary material.

Acknowledgments

We thank Dr. Arthur Spector for helpful comments on the manuscript. This work was supported by the Intramural Research Program of the National Institute of Alcohol Abuse and Alcoholism, National Institutes of Health.

Abbreviations

AEA	anandamide
AA	arachidonic acid
bFGF	basic fibroblast growth factor
BDNF	brain derived neurotrophic factor

BSA	bovine serum albumin
CREB	cAMP response element binding protein
CB1	cannabinoid receptor type 1
DAPI	4 ,6-diamidino-2-phenylindole
DHA	docosahexaenoic acid
DPAn-6	docosapentaenoic acid
DMEM/F12	Dulbecco's Modified Eagle Medium/Ham'a F12
FAAH	fatty acid amide hydrolase
GAPDH	glyceraldehyde 3-phosphate dehydrogenase
GFAP	glial fibrillary acidic protein
GPR	G protein coupled receptor
GFP	green fluorescent protein
MH+	protonated molecular ion
NAE	N-acylethanolamines
MAP2	microtubule-associated protein 2
NSCs	neural stem cells
Tuj-1	neuron-specific class III beta-tubulin
OA	oleic acid
PPARs	peroxisome proliferator-activated receptors
PUFA	polyunsaturated fatty acids
PVDF	polyvinylidene difluoride
PKA	protein kinase A
RXR	retinoid X receptor
shRNA	small hairpin RNA
TBS	Tris-buffered solution

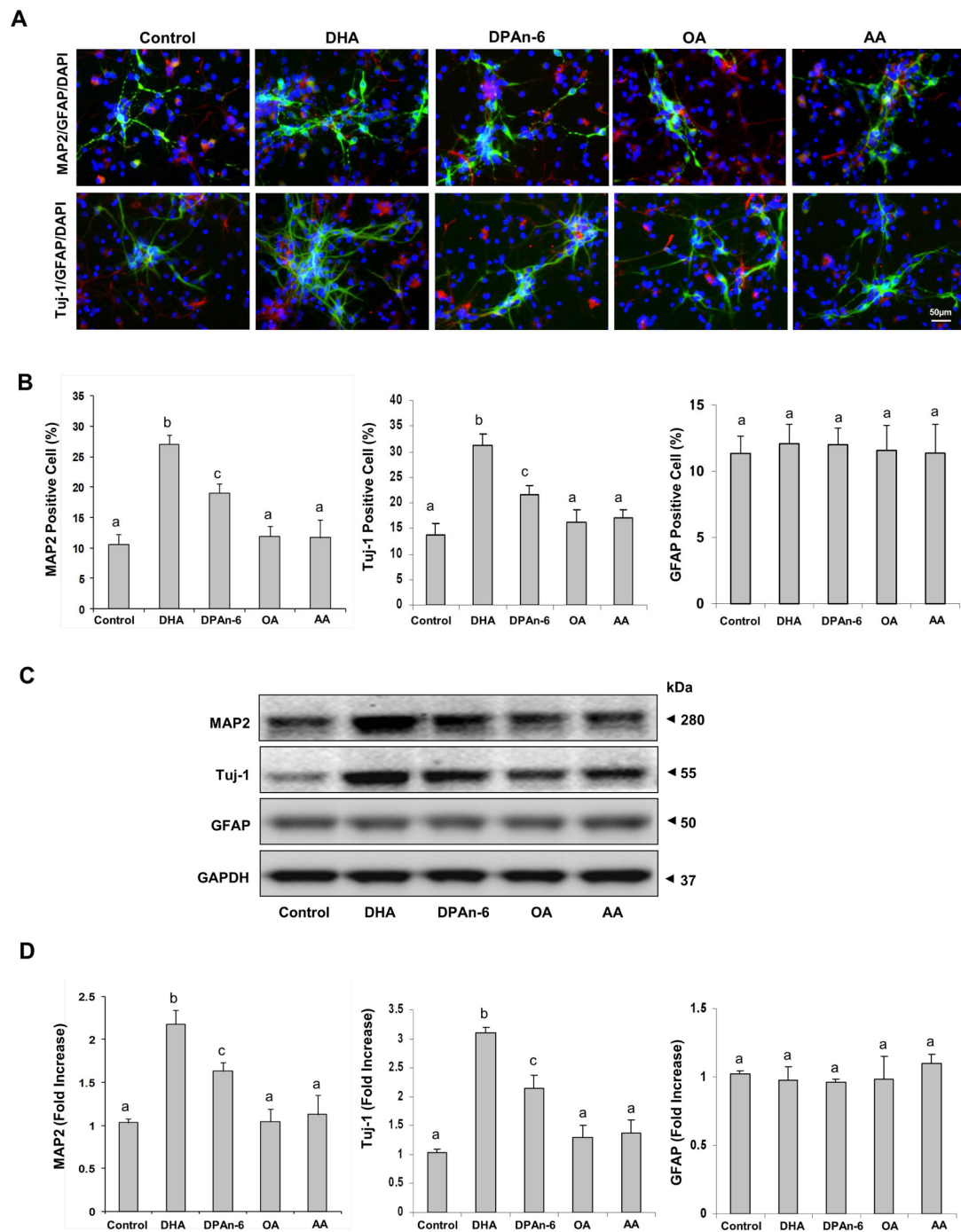
References

- Akbar M, Calderon F, Wen Z, Kim HY. Docosahexaenoic acid: a positive modulator of Akt signaling in neuronal survival. *Proc Natl Acad Sci USA*. 2005; 102:10858–10863. [PubMed: 16040805]
- Artmann A, Petersen G, Hellgren LI, Boberg J, Skonberg C, Nellemann C, Hansen SH, Hansen HS. Influence of dietary fatty acids on endocannabinoid and N-acylethanolamine levels in rat brain, liver and small intestine. *Biochim Biophys Acta*. 2008; 1781:200–212. [PubMed: 18316044]
- Bazan NG. Cell survival matters: docosahexaenoic acid signaling, neuroprotection and photoreceptors. *Trends Neurosci*. 2006; 29:263–271. [PubMed: 16580739]
- Berger A, Crozier G, Bisogno T, Cavaliere P, Innis S, Di Marzo V. Anandamide and diet: inclusion of dietary arachidonate and docosahexaenoate leads to increased brain levels of the corresponding N-acylethanolamines in piglets. *Proc Natl Acad Sci USA*. 2001; 98:6402–6406. [PubMed: 11353819]
- Bi Y, Gong M, Zhang X, Zhang X, Jiang W, Zhang Y, Chen J, Liu Y, He TC, Li T. Pre-activation of retinoid signaling facilitates neuronal differentiation of mesenchymal stem cells. *Dev Growth Differ*. 2010; 52:419–431. [PubMed: 20507357]

- Bligh EG, Dyer WJ. A rapid method of total lipid extraction and purification. *Can J Med Sci.* 1959; 37:911–917.
- Calderon F, Kim HY. Docosahexaenoic acid promotes neurite growth in hippocampal neurons. *J Neurochem.* 2004; 90:979–988. [PubMed: 15287904]
- Calderon F, Kim HY. Role of RXR in neurite outgrowth induced by docosahexaenoic acid. *Prostaglandins Leukot Essent Fatty Acids.* 2007; 77:227–232. [PubMed: 18036800]
- Cao D, Kevala K, Kim J, Moon HS, Jun SB, Lovinger D, Kim HY. Docosahexaenoic acid promotes hippocampal neuronal development and synaptic function. *J Neurochem.* 2009; 111:510–521. [PubMed: 19682204]
- Chu MS, Chang CF, Yang CC, Bau YC, Ho LL, Hung SC. Signaling pathway in the induction of neurite outgrowth in human mesenchymal stem cells. *Cell Signal.* 2006; 18:519–530. [PubMed: 16098715]
- Cimini A, Ceru MP. Emerging roles of peroxisome proliferator-activated receptors (PPARs) in the regulation of neural stem cells proliferation and differentiation. *Stem Cell Rev.* 2008; 4:293–303. [PubMed: 18561036]
- Connor M, Vaughan CW, Vandenberg RJ. N-acyl amino acids and N-acyl neurotransmitter conjugates: neuromodulators and probes for new drug targets. *Br J Pharmacol.* 2010; 160:1857–1871. [PubMed: 20649585]
- Contreras MA, Greiner RS, Chang MC, Myers CS, Salem N Jr, Rapoport SI. Nutritional deprivation of alpha-linolenic acid decreases but does not abolish turnover and availability of unacylated docosahexaenoic acid and docosahexaenoyl-CoA in rat brain. *J Neurochem.* 2000; 75:2392–2400. [PubMed: 11080190]
- Cravatt BF, Demarest K, Patricelli MP, Bracey MH, Giang DK, Martin BR, Lichtman AH. Supersensitivity to anandamide and enhanced endogenous cannabinoid signaling in mice lacking fatty acid amide hydrolase. *Proc Natl Acad Sci USA.* 2001; 98:9371–9376. [PubMed: 11470906]
- de Urquiza AM, Liu S, Sjoberg M, Zetterstrom RH, Griffiths W, Sjoval J, Perlmann T. Docosahexaenoic acid, a ligand for the retinoid X receptor in mouse brain. *Science.* 2000; 290:2140–2144. [PubMed: 11118147]
- Galli C, Trzeciak HI, Paoletti R. Effects of dietary fatty acids on the fatty acid composition of brain ethanolamine phosphoglyceride: reciprocal replacement of n-6 and n-3 polyunsaturated fatty acids. *Biochim Biophys Acta.* 1971; 248:449–454.
- He C, Qu X, Cui L, Wang J, Kang JX. Improved spatial learning performance of fat-1 mice is associated with enhanced neurogenesis and neuritogenesis by docosahexaenoic acid. *Proc Natl Acad Sci USA.* 2009; 106:11370–11375. [PubMed: 19549874]
- Jagasia R, Steib K, Englberger E, Herold S, Faus-Kessler T, Saxe M, Gage FH, Song H, Lie DC. GABA-cAMP response element-binding protein signaling regulates maturation and survival of newly generated neurons in the adult hippocampus. *J Neurosci.* 2009; 29:7966–7977. [PubMed: 19553437]
- Jiang W, Zhang Y, Xiao L, Van Cleemput J, Ji SP, Bai G, Zhang X. Cannabinoids promote embryonic and adult hippocampus neurogenesis and produce anxiolytic- and antidepressant-like effects. *J Clin Invest.* 2005; 115:3104–3116. [PubMed: 16224541]
- Johannessen M, Delghandi MP, Moens U. What turns CREB on? *Cell Signal.* 2004; 16:1211–1227. [PubMed: 15337521]
- Katakura M, Hashimoto M, Shahdat HM, Gamoh S, Okui T, Matsuzaki K, Shido O. Docosahexaenoic acid promotes neuronal differentiation by regulating basic helix-loop-helix transcription factors and cell cycle in neural stem cells. *Neuroscience.* 2009; 160:651–660. [PubMed: 19272428]
- Kawakita E, Hashimoto M, Shido O. Docosahexaenoic acid promotes neurogenesis in vitro and in vivo. *Neuroscience.* 2006; 139:991–997. [PubMed: 16527422]
- Kim G, Choe Y, Park J, Cho S, Kim K. Activation of protein kinase A induces neuronal differentiation of HiB5 hippocampal progenitor cells. *Brain Res Mol Brain Res.* 2002; 109:134–145. [PubMed: 12531523]
- Kim HY, Akbar M, Lau A, Edsall L. Inhibition of neuronal apoptosis by docosahexaenoic acid (22:6n-3): role of phosphatidylserine in antiapoptotic effect. *J Biol Chem.* 2000; 275:35215–35223. [PubMed: 10903316]

- Kim HY, Akbar M, Kim YS. Phosphatidylserine-dependent neuroprotective signaling promoted by docosahexaenoic acid. *Prostaglandins Leukot Essent Fatty Acids*. 2010; 82:165–172. [PubMed: 20207120]
- Kim HY, Moon HS, Cao D, Lee J, Kevala K, Jun S, Lovinger D, Akbar M, Huang BX. N-Docosahexaenoyl ethanolamide promotes development of hippocampal neurons. *Biochem J*. 2011a; 96:114–120.
- Kim HY, Spector AA, Xiong ZM. A synaptogenic amide N-docosahexaenoyl ethanolamide promotes hippocampal development. *Prostaglandins Other Lipid Mediat*. 2011b; 96:114–120. [PubMed: 21810478]
- Korchev YE, Gorelik J, Lab MJ, Sviderskaya EV, Johnston CL, Coombes CR, Vodyanoy I, Edwards CR. Cell volume measurement using scanning ion conductance microscopy. *Biophys J*. 2000; 78:451–457. [PubMed: 10620308]
- Lee E, Son H. Adult hippocampal neurogenesis and related neurotrophic factors. *BMB Rep*. 2009; 42:239–244. [PubMed: 19470236]
- Lee JE. NeuroD and neurogenesis. *Dev Neurosci*. 1997; 19:27–32. [PubMed: 9078430]
- Lengqvist J, Mata De Urquiza A, Bergman AC, Willson TM, Sjoval J, Perlmann T, Griffiths WJ. Polyunsaturated fatty acids including docosahexaenoic and arachidonic acid bind to the retinoid X receptor alpha ligand-binding domain. *Mol Cell, Proteomics*. 2004; 3:692–703. [PubMed: 15073272]
- Lepski G, Jannes CE, Maciaczyk J, Papazoglou A, Mehlhorn AT, Kaiser S, Teixeira MJ, Marie SK, Bischofberger J, Nikkhah G. Limited Ca²⁺ and PKA-pathway dependent neurogenic differentiation of human adult mesenchymal stem cells as compared to fetal neuronal stem cells. *Exp Cell Res*. 2010; 316:216–231. [PubMed: 19686736]
- Lim SY, Hoshiba J, Salem N Jr. An extraordinary degree of structural specificity is required in neural phospholipids for optimal brain function: n-6 docosapentaenoic acid substitution for docosahexaenoic acid leads to a loss in spatial task performance. *J Neurochem*. 2005; 95:848–857. [PubMed: 16135079]
- Lonze BE, Ginty DD. Function and regulation of CREB family transcription factors in the nervous system. *Neuron*. 2002; 35:605–623. [PubMed: 12194863]
- Ma D, Zhang M, Larsen CP, Xu F, Hua W, Yamashima T, Mao Y, Zhou L. DHA promotes the neuronal differentiation of rat neural stem cells transfected with GPR40 gene. *Brain Res*. 2010; 1330:1–8. [PubMed: 20211608]
- Ma D, Lu L, Boneva NB, Warashina S, Kaplamadzhiev DB, Mori Y, Nakaya MA, Kikuchi M, Tonchev AB, Okano H, Yamashima T. Expression of free fatty acid receptor GPR40 in the neurogenic niche of adult monkey hippocampus. *Hippocampus*. 2008; 18:326–333. [PubMed: 18064707]
- McNamara RK, Carlson SE. Role of omega-3 fatty acids in brain development and function: potential implications for the pathogenesis and prevention of psychopathology. *Prostaglandins Leukot Essent Fatty Acids*. 2006; 75:329–349. [PubMed: 16949263]
- Morales-Garcia JA, Luna-Medina R, Alfaro-Cervello C, Cortes-Canteli M, Santos A, Garcia-Verdugo JM, Perez-Castillo A. Peroxisome proliferator-activated receptor gamma ligands regulate neural stem cell proliferation and differentiation in vitro and in vivo. *Glia*. 2011; 59:293–307. [PubMed: 21125653]
- Moriguchi T, Greiner RS, Salem N Jr. Behavioral deficits associated with dietary induction of decreased brain docosahexaenoic acid concentration. *J Neurochem*. 2000; 75:2563–2573. [PubMed: 11080210]
- Palmer TD, Takahashi J, Gage FH. The adult rat hippocampus contains primordial neural stem cells. *Mol Cell Neurosci*. 1997; 8:389–404. [PubMed: 9143557]
- Parikh K, Peppelenbosch MP, Ritsema T. Kinome profiling using peptide arrays in eukaryotic cells. *Methods Mol Biol*. 2009; 527:269–280. [PubMed: 19241020]
- Rietze RL, Reynolds BA. Neural stem cell isolation and characterization. *Methods Enzymol*. 2006; 419:3–23. [PubMed: 17141049]

- Sakayori N, Maekawa M, Numayama-Tsuruta K, Katura T, Moriya T, Osumi N. Distinctive effects of arachidonic acid and docosahexaenoic acid on neural stem /progenitor cells. *Genes Cells*. 2011; 16:778–790. [PubMed: 21668588]
- Salem N Jr, Litman B, Kim HY, Gawrisch K. Mechanisms of action of docosahexaenoic acid in the nervous system. *Lipids*. 2001; 36:945–959. [PubMed: 11724467]
- Sheskin T, Hanus L, Slager J, Vogel Z, Mechoulam R. Structural requirements for binding of anandamide-type compounds to the brain cannabinoid receptor. *J Med Chem*. 1997; 40:659–667. [PubMed: 9057852]
- Sidhu VK, Huang BX, Kim HY. Effects of docosahexaenoic acid on mouse brain synaptic plasma membrane proteome analyzed by mass spectrometry and (16)O/(18)O labeling. *J Proteome Res*. 2011; 10:5472–5480. [PubMed: 22003853]
- Soltys J, Yushak M, Mao-Draayer Y. Regulation of neural progenitor cell fate by anandamide. *Biochem Biophys Res Commun*. 2010; 400:21–26. [PubMed: 20691161]
- Wada K, Nakajima A, Katayama K, Kudo C, Shibuya A, Kubota N, Terauchi Y, Tachibana M, Miyoshi H, Kamisaki Y, Mayumi T, Kadowaki T, Blumberg RS. Peroxisome proliferator-activated receptor gamma-mediated regulation of neural stem cell proliferation and differentiation. *J Biol Chem*. 2006; 281:12673–12681. [PubMed: 16524877]
- Wang B, McVeagh P, Petocz P, Brand-Miller J. Brain ganglioside and glycoprotein sialic acid in breastfed compared with formula-fed infants. *Am J Clin Nutr*. 2003; 78:1024–1029. [PubMed: 14594791]
- Wen Z, Kim HY. Alterations in hippocampal phospholipid profile by prenatal exposure to ethanol. *J Neurochem*. 2004; 89:1368–1377. [PubMed: 15189339]
- Wu A, Ying Z, Gomez-Pinilla F. The salutary effects of DHA dietary supplementation on cognition, neuroplasticity, and membrane homeostasis after brain trauma. *J Neurotrauma*. 2011; 28:2113–2122. [PubMed: 21851229]

**Figure 1.**

Effects of long chain PUFA on differentiation of NSCs. NSCs were treated with 1 μM long chain PUFA bound to 0.05% BSA for 7 days and subjected to immunofluorescence and western blot analyses. NSCs were stained for MAP2 (green, mature neuron marker), Tuj-1 (green, early neuron marker), GFAP (red, glia marker) and nuclei (blue, DAPI), and visualized by fluorescence microscopy (A). The percentage of Tuj-1 and GFAP positive cells was evaluated using MetaMorph software (B). Western blot analysis was performed for MAP2, Tuj-1 and GFAP (C) and quantified by densitometry (D). The data are expressed as

the mean \pm SD of triplicates or quadruplicates, representing three to four independent experiments. ^{a-c}, Bars with different letter superscripts are significantly different (Bonferroni's multiple comparison test, $p < 0.01$).

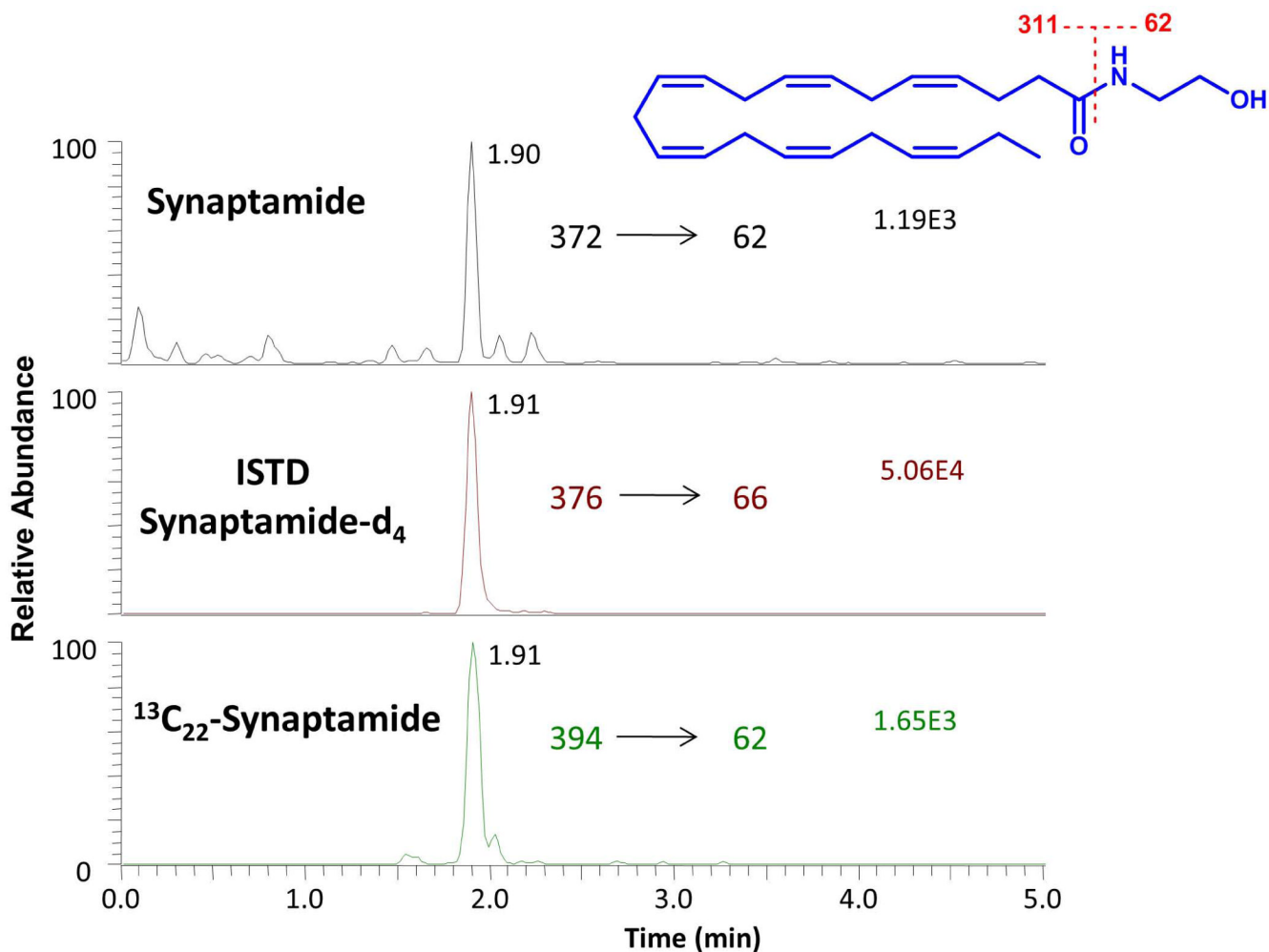


Figure 2. Identification of synaptamide production from DHA by NSCs. NSCs were incubated with 1 μ M DHA and $^{13}\text{C}_{22}$ -DHA for 4 days under a differentiating condition (in the absence of FGF). Lipids were extracted from the cultures and analyzed by mass spectrometry for synaptamide using MRM. Both non-labeled and $^{13}\text{C}_{22}$ -labeled synaptamide were detected at the same retention time, indicating that DHA and $^{13}\text{C}_{22}$ -DHA were metabolized to synaptamide by NSCs. Synaptamide-d₄ was used as an internal standard.

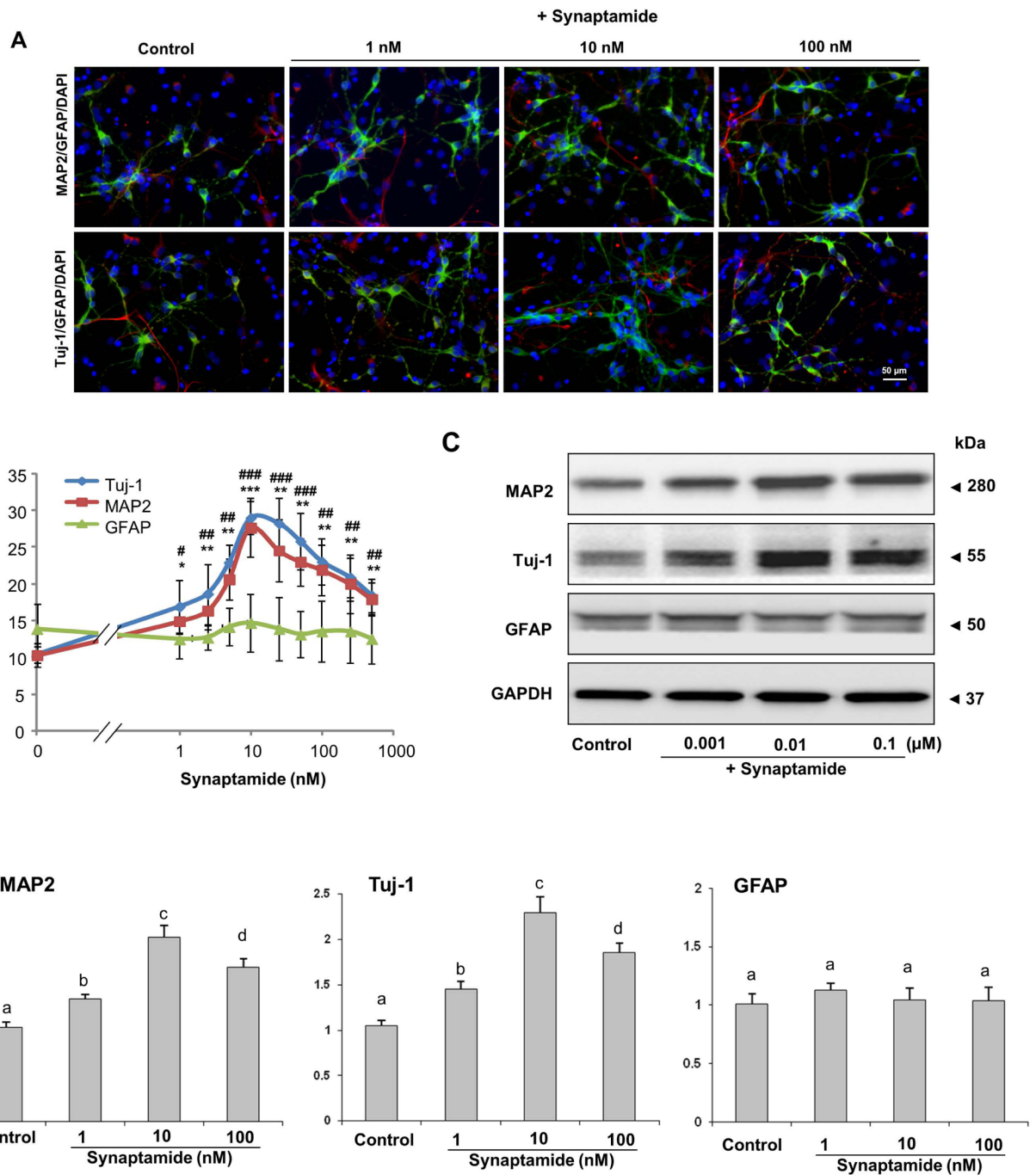


Figure 3. Induction of neuronal differentiation of NSCs by synaptamide. NSCs were treated with various concentrations of synaptamide for 7 days, stained for MAP2 (green), Tuj-1 (green), GFAP (red) and DAPI (nuclei), and visualized by fluorescence microscopy (A), and the percentage of MAP2, Tuj-1 and GFAP positive cells was evaluated using MetaMorph software in the 1–500 nM range (B). Effects of synaptamide on the expression of MAP2, Tuj-1 and GFAP for selected concentrations were evaluated by western blot (C) which was quantified by densitometry (D). Representative photomicrographs (A) and western blot data (C, D) are shown for 1, 10 and 100 nM concentrations. The data are expressed as the mean \pm

SD of triplicates, and represent at least three independent experiments. *, $p < 0.05$; **, $p < 0.01$; ***, $p < 0.001$; #, $p < 0.05$; ##, $p < 0.01$; ###, $p < 0.001$ for Tuj-1 (*) and MAP2-positive cells (#) compared to vehicle control. ^{a-c}, Bars with different letter superscripts are significantly different (Bonferroni's multiple comparison test, $p < 0.01$).

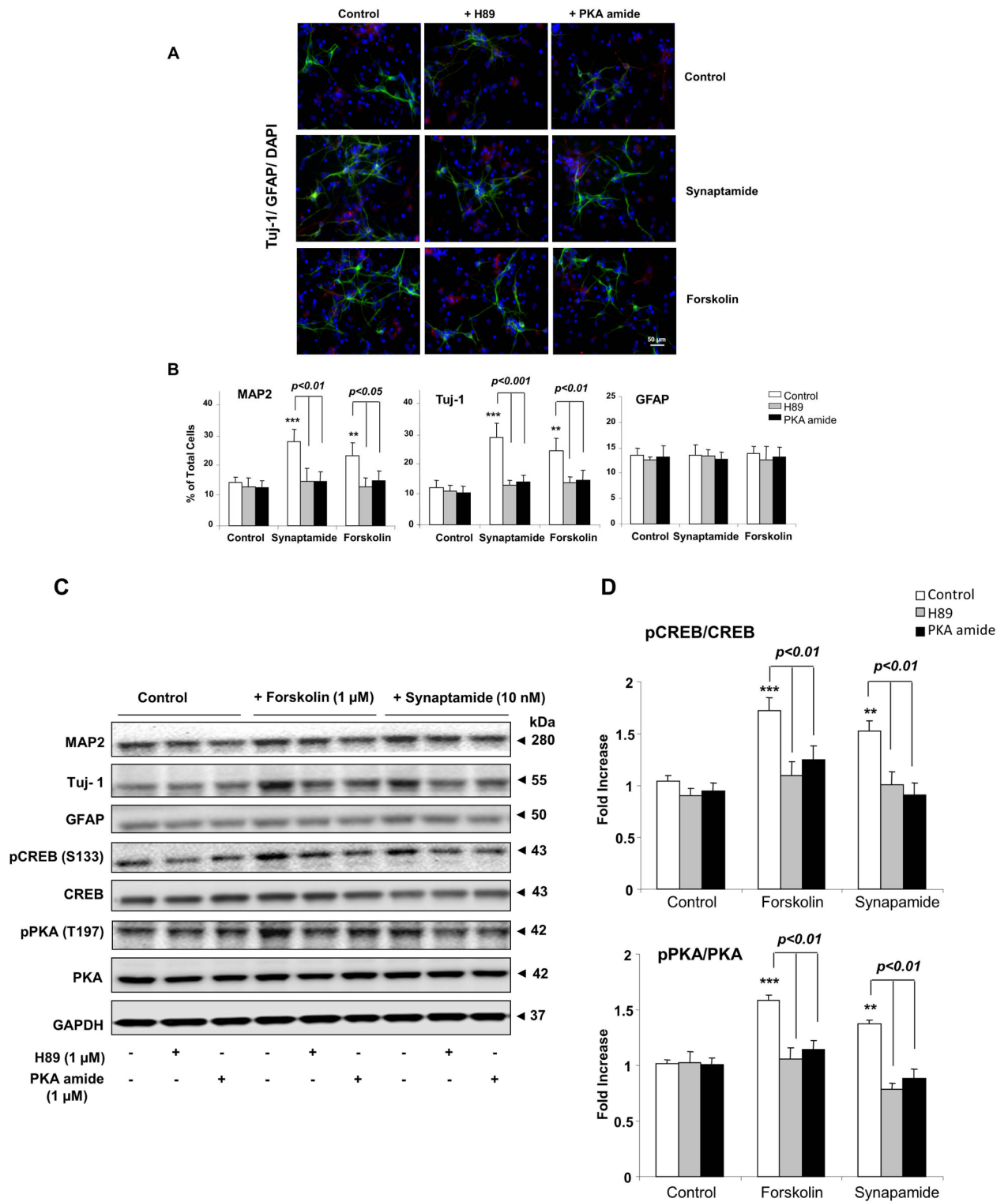
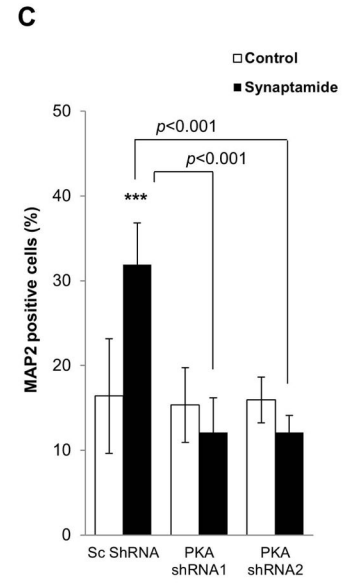
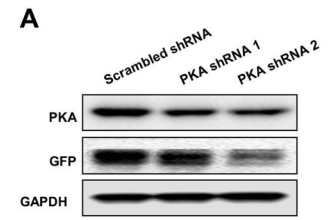
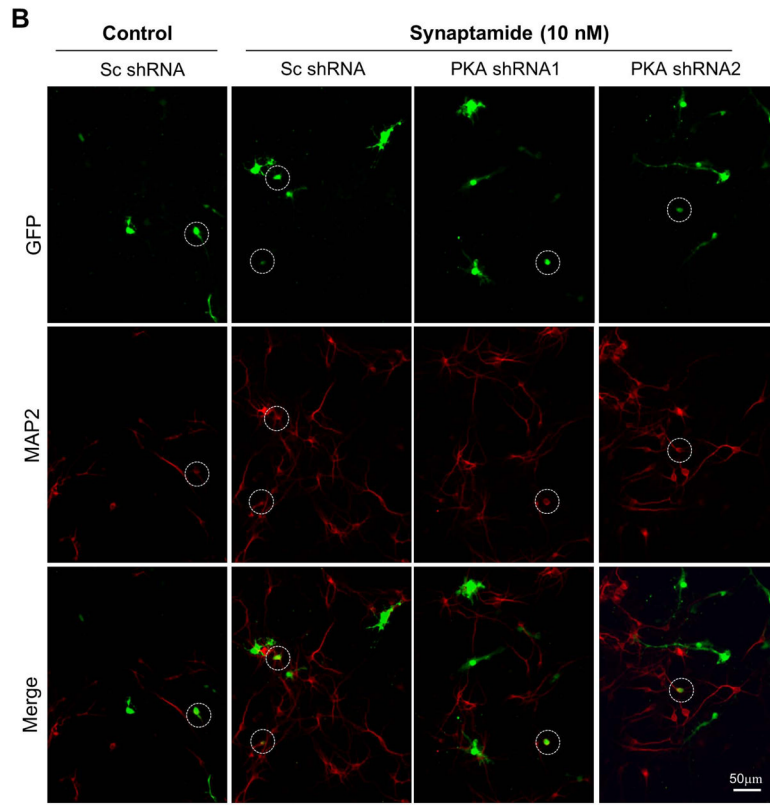


Figure 4. Critical role of PKA/CREB activation in synaptamide-induced neuronal differentiation of NSCs. NSCs were treated with PKA inhibitor, H89 (1 μ M) or PKA inhibitor 6–22 amide (1 μ M) for 30 min, and then incubated with synaptamide (10 nM) or forskolin (1 μ M) for 7

days. NSCs cells were stained for Tuj-1 (green), GFAP (red) and nuclei (DAPI), and visualized by fluorescence microscopy (A), and the percentage of Tuj-1 and GFAP positive cells was evaluated using MetaMorph software (B). Western blot analysis was performed for CREB and PKA phosphorylation along with MAP2, Tuj-1 and GFAP (C). Phosphorylated CREB and PKA level was normalized to the total CREB and total PKA, respectively, and compared to their basal levels (D). Micrographs for MAP2 staining are not shown. The data are expressed as the mean \pm SD of triplicates, representing three independent experiments. **, $p < 0.01$; ***, $p < 0.001$ compared to DMSO control.



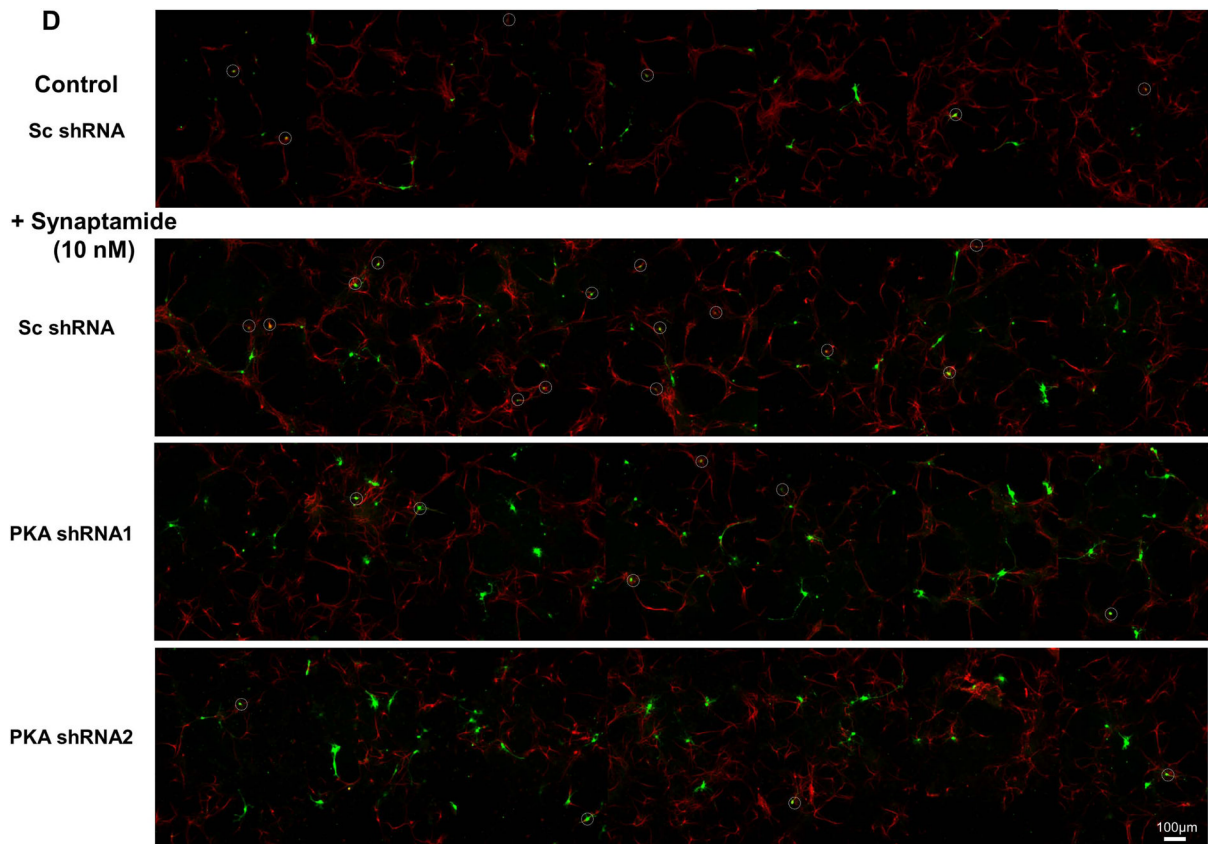
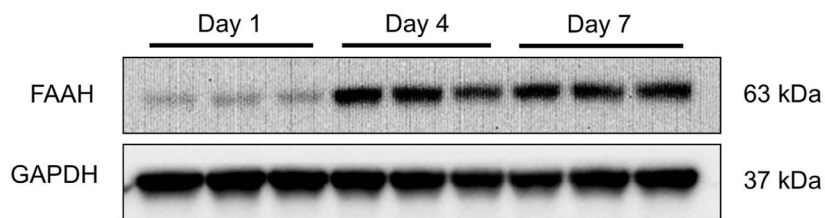
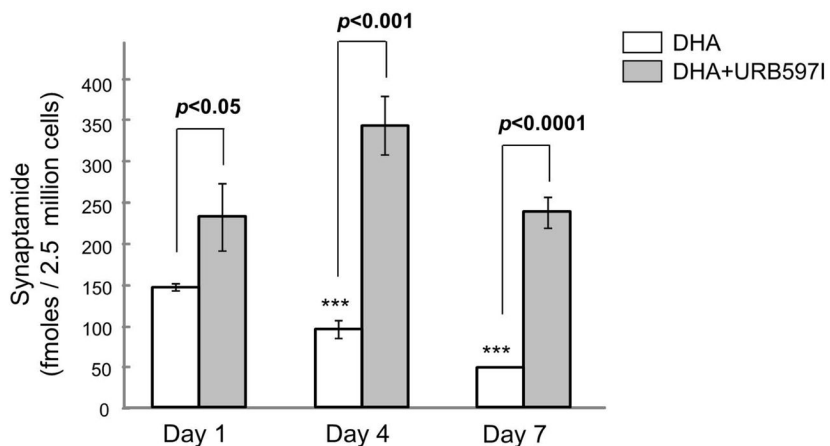
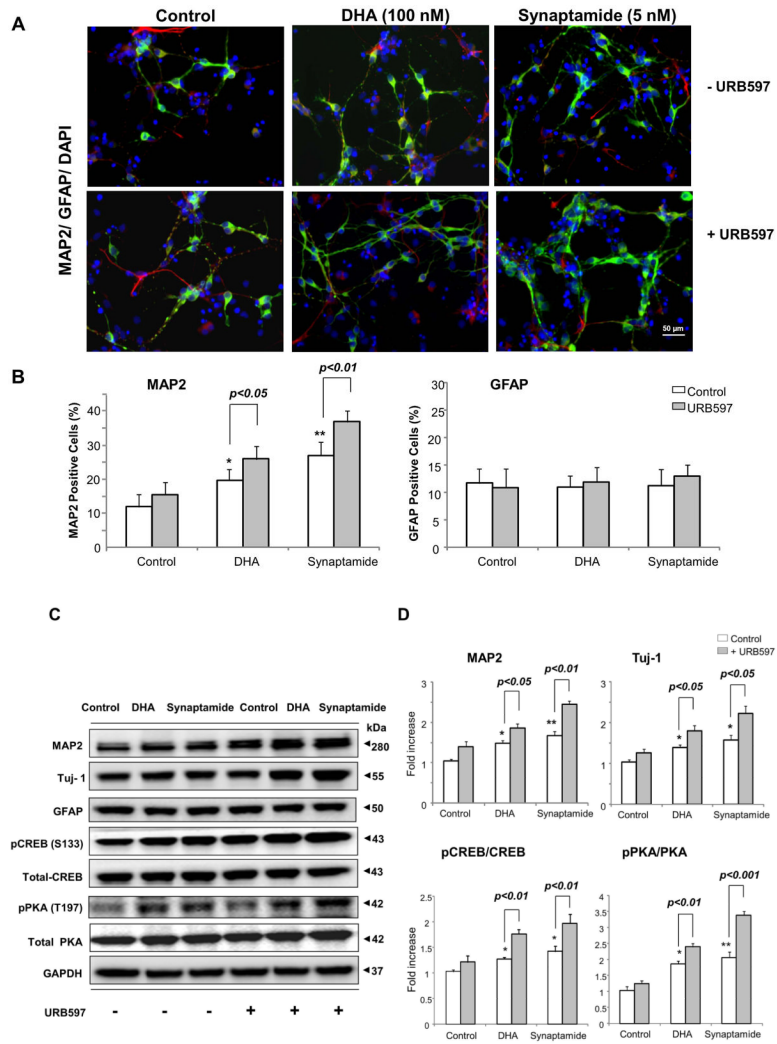


Figure 5.

Inhibition of synaptamide-induced neuronal differentiation of NSCs by PKA knockdown. NSCs were transfected on the 4th day of culture under differentiation condition with GFP-coexpressing scrambled shRNA (Sc) or shRNA targeting PKA catalytic subunit (0.8 μ g of plasmid DNA/ 5×10^6 cells). After 4 h, the transfection medium was removed and NSCs were treated with vehicle (DMSO control) or 10 nM synaptamide for the next 72h. (A) Western blot analysis confirming effectiveness of shRNAs in suppressing PKA expression. Decreased PKA expression is clearly indicated after Neuro 2A cells were transfected with shRNAs for 24 h. (B) Representative photomicrographs showing the GFP-tagged shRNA transfected cells (green) and neurons stained with MAP2 (red). Cells which are both MAP2- and GFP-positive are displayed as orange and marked with circles. (C) Quantitative results indicating that synaptamide-induced neuronal differentiation was significantly decreased by PKA shRNA transfection. (D) Representative photomicrographs with lower magnification (X10) showing that synaptamide-induced neuronal differentiation of NSCs is blocked by PKA knockdown. Two separate PKA shRNA plasmids produced similar inhibition. The quantified values represent the percent of MAP2 positive cells detected among at least 100 GFP-positive transfected cells per sample, and are averages of results from three independent experiments \pm SD. ***, $p < 0.001$ compared to DMSO control.

A**B****Figure 6.**

Effects of FAAH on synaptamide levels during NSC differentiation. (A) The FAAH protein expression profile during NSC differentiation evaluated by western blot analysis. (B) Synaptamide levels quantified by mass spectrometry after NSCs were supplemented with 1 μ M DHA with or without 20 nM URB5971 for the indicated time period during differentiation. The data are expressed as the mean \pm SD of triplicates, representing three independent experiments. ***, $p < 0.001$ compared to the synaptamide level on day 1.



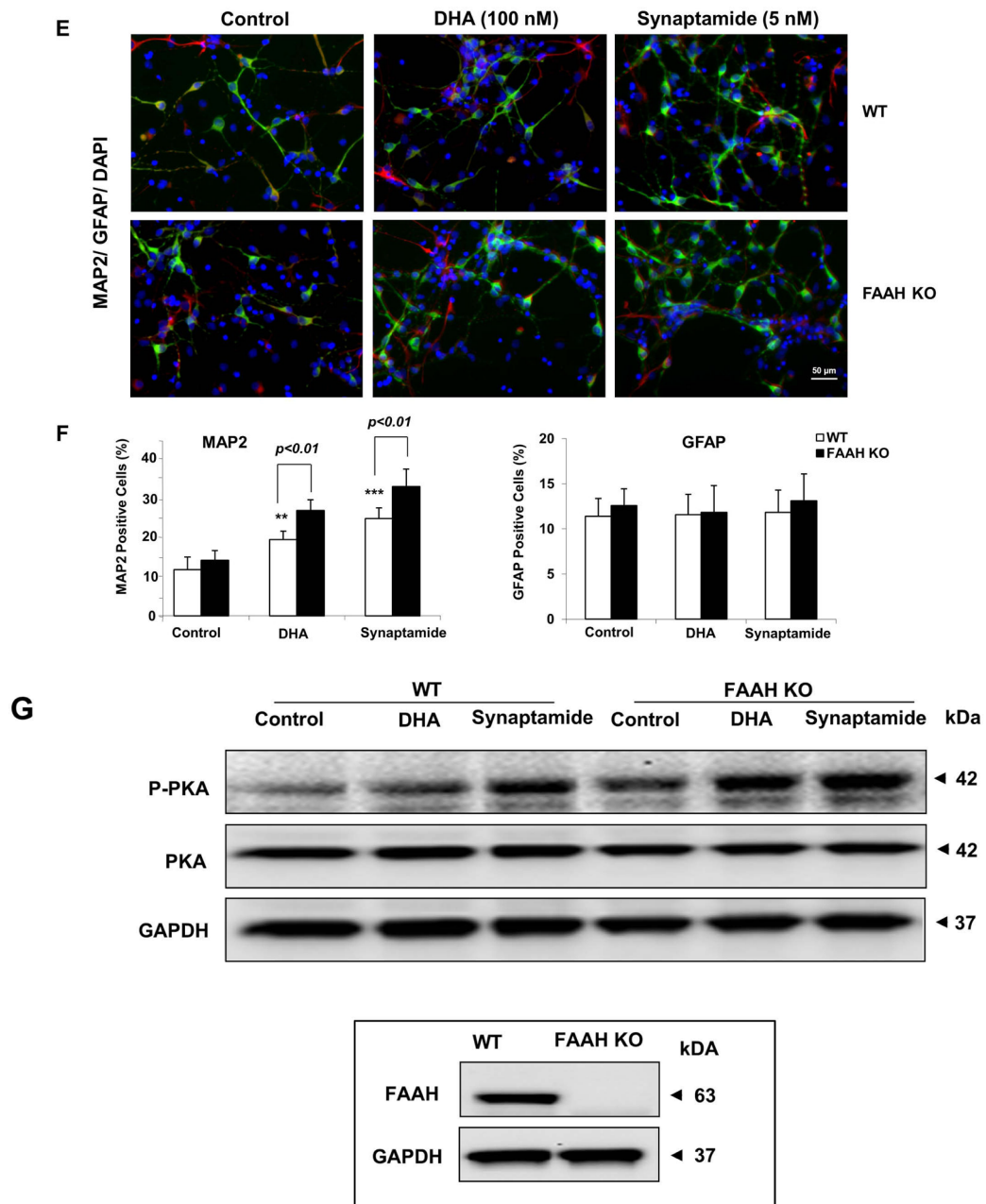


Figure 7.

Effects of FAAH suppression on neuronal differentiation of NSCs. NSCs were treated with URB597 (20 nM) for 30 min, and then with synaptamide (5 nM) or DHA (100 nM) for 7 days. NSCs were stained for MAP2 (green), GFAP (red) and nuclei (DAPI), and visualized by fluorescence microscopy (A). Percentages of MAP2 and GFAP positive cells were evaluated using MetaMorph software (B). The protein levels of MAP2, Tuj-1 and GFAP, pCREB and pPKA were evaluated by western blot analysis (C) and quantified by densitometry (D). The NSCs from FAAH KO mice showed increased capacity for DHA- or synaptamide-induced neuronal differentiation as indicated by the representative photomicrographs (E) and quantification of MAP2-positive cells (F), along with enhanced PKA phosphorylation detected by western blot analysis (F). Inset: Absence of FAAH protein expression in FAAH KO mice. WT: wild type. The data are expressed as the mean \pm

SD of triplicates representing two independent experiments. *, $p < 0.05$ **; $p < 0.01$; ***, $p < 0.001$ compared to DMSO control.

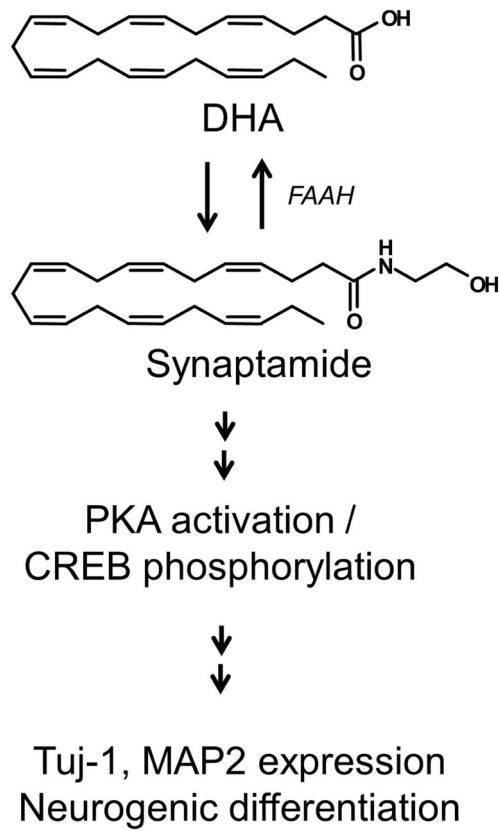


Figure 8.
Scheme for DHA-induced neural stem cell differentiation into neurons